Available online at www.sciencedirect.com
ScienceDirect
Inorganica Chimica Acta 361 (2008) 2285–2295
Inorganica Chimica Acta
www.elsevier.com/locate/ica

Methyl iodide oxidative addition to monocarbonylphosphine [Rh((C$_4$H$_3$S)COCHCOR)(CO)(PPh$_3$)] complexes utilizing UV/vis and IR spectrophotometry and NMR spectroscopy to identify reaction intermediates: R = C$_6$H$_5$ or C$_4$H$_3$S

Marrigje M. Conradie, Jeanet Conradie *

Department of Chemistry, University of the Free State, Bloemfontein, Free State 9301, South Africa

Received 4 September 2007; received in revised form 25 October 2007; accepted 26 October 2007
Available online 4 December 2007

Abstract

The chemical kinetics, studied by UV/vis and IR, of the oxidative addition of CH_3I to [Rh((C$_4$H$_3$S)COCHCOR)(CO)(PPh$_3$)], with R = C$_6$H$_5$ (Ph) or C$_4$H$_3$S, consists of three definite reaction steps and involves isomers of two distinctly different classes of a Rh^{III}-alkyl and two distinctly different classes of a Rh^{III}–acyl species according to the following reaction scheme:

$$Rh^{I} + CH_3I \underset{k_{-1}}{\overset{K_1, k_1}{\rightleftharpoons}} \{\, Rh^{III}\text{-alkyl1} \underset{k_{-2}}{\overset{K_2, k_2}{\rightleftharpoons}} [Rh^{III}\text{-acyl1}] \,\} \underset{k_{-3}}{\overset{k_3}{\rightleftharpoons}} [Rh^{III}\text{-alkyl2}] \underset{k_{-4}}{\overset{k_4}{\rightleftharpoons}} [Rh^{III}\text{-acyl2}]$$

The molecular formulas of all the Rh^{III}–alkyl and Rh^{III}–acyl species are [Rh((C$_4$H$_3$S)COCHCOR)(CH$_3$)(CO)(PPh$_3$)(I)] and [Rh((C$_4$H$_3$S)COCHCOR)(COCH$_3$)(PPh$_3$)(I)] respectively, but the geometry is different due to different co-ordination positions of the ligands. The equilibrium K_2 was fast enough to be maintained during the Rh^{I} depletion in the first reaction step and during the Rh^{III}–alkyl2 formation in the second reaction step. A ^{1}H and ^{31}P NMR study of the oxidative addition of CH_3I to the different isomers of [Rh((C$_4$H$_3$S)COCHCOC$_6$H$_5$)(CO)(PPh$_3$)], containing an unsymmetrical β-diketonato ligand, reveals the existence of at least two structural isomers for each reaction intermediate according to the following reaction scheme:

$$\begin{bmatrix} Rh^{I}\text{-A} \\ \uparrow\downarrow K_{c1} \\ Rh^{I}\text{-B} \end{bmatrix} + CH_3I \underset{k_{-1}}{\overset{K_1, k_1}{\rightleftharpoons}} \begin{bmatrix} [Rh^{III}\text{-alkyl1A}] \\ \uparrow\downarrow K_{c2} \\ [Rh^{III}\text{-alkyl1B}] \end{bmatrix} \underset{k_{-2}}{\overset{K_2, k_2}{\rightleftharpoons}} \begin{bmatrix} [Rh^{III}\text{-acyl1A}] \\ \uparrow\downarrow K_{c3} \\ [Rh^{III}\text{-acyl1B}] \end{bmatrix} \underset{k_{-3}}{\overset{k_3}{\rightleftharpoons}} \begin{bmatrix} [Rh^{III}\text{-alkyl2A}] \\ \uparrow\downarrow K_{c4} \\ [Rh^{III}\text{-alkyl2B}] \end{bmatrix} \underset{k_{-4}}{\overset{k_4}{\rightleftharpoons}} \begin{bmatrix} [Rh^{III}\text{-acyl2A}] \\ \uparrow\downarrow K_{c5} \\ [Rh^{III}\text{-acyl2B}] \end{bmatrix}$$

The observed rate of formation and depletion of the two Rh^{I} isomers of the [Rh((C$_4$H$_3$S)COCHCO(C$_6$H$_5$))(CO)(PPh$_3$)] complex, as well as the different isomers of each reaction intermediate, are the same, contrary to what was previously found for the formation of the alkyl2 isomers when R = CF$_3$. All reaction intermediates are identified spectroscopically.

Keywords: β-Diketonate; Thienyl; Rhodium; Oxidative addition; NMR; Carbonyl; Phosphine

1. Introduction

The interaction of square planar rhodium(I) complexes with methyl iodide keeps drawing attention as a simple

* Corresponding author. Tel.: +27 51 4012194; fax: +27 51 4446384.
E-mail address: conradj.sci@ufs.ac.za (J. Conradie).

0020-1693/$ - see front matter © 2007 Elsevier B.V. All rights reserved.
doi:10.1016/j.ica.2007.10.052

and convenient model of the reaction of oxidative addition, one of the key stages of important catalytic processes such as the methanol carbonylation to acetic acid in the presence of $[Rh(CO)_2I_2]^-$ (Monsanto process) [1]. Although the first reaction product of the carbonyl-containing square planar $[Rh^I(L,L'\text{-BID})(CO)(PPh_3)]$ complexes (L,L′-BID = monoanionic bidentate ligand with donor atoms L and L′, Ph = C_6H_5) with methyl iodide is a Rh^{III}–alkyl species, mechanistic concepts suggest in many cases that the oxidative addition reaction proceeds through Rh^{III}–alkyl and Rh^{III} –acyl intermediates. The final or most stable reaction products that form are octahedral or square-pyramidal complexes of rhodium(III) with different mutual disposition of the ligands [2–11]. For instance, the final reaction product of the oxidative addition reaction of methyl iodide to a series square planar $[Rh^I(L,L'\text{-BID})(CO)(PPh_3)]$ complexes, with L and L′ = O,O [5], O,N [11] O,S [11,12] and N,S [11,13], is a Rh^{III}–acyl species $[Rh^{III}(L,L'\text{-BID})(COCH_3)(PPh_3)(I)]$. Oxidative addition of methyl iodide to a series of square planar $[Rh^I(\beta\text{-diketonato})(CO)(PPh_3)]$ complexes yield an Rh^{III}–alkyl species $[Rh^{III}(\beta\text{-diketonato})(CH_3)(CO)(PPh_3)(I)]$ as the final reaction product [14–16]. Recently it has been shown that for the oxidative addition of methyl iodide to $[Rh(fctfa)(CO)(PPh_3)]$ with Hfctfa = ferrocenoyltrifluoroacetone, another reaction step, involving the formation of a second Rh^{III}–acyl species, has been observed [17]. Reaction 1 summarizes the general mechanism for the oxidative addition of methyl iodide to square planar rhodium(I) complexes containing a monoanionic bidentate ligand. The first alkyl species in reaction 1 may involve an ionic intermediate $[Rh^{III}(L,L'\text{-BID})(CH_3)(CO)(PPh_3)]^+(I)^-$ [14,12,18] or a solvent pathway [11].

$$[Rh^I(L,L'\text{-BID})(CO)(PPh_3)] + CH_3I \underset{k_{-1}}{\overset{K_1,k_1}{\rightleftharpoons}} \text{alkyl1} \underset{k_{-2}}{\overset{k_2}{\rightleftharpoons}} \text{acyl1} \underset{k_{-3}}{\overset{k_3}{\rightleftharpoons}} \underset{\text{product for acac, tfaa, tfdma, hfaa, sacac, tta}}{\text{alkyl2}} \underset{k_{-4}}{\overset{k_4}{\rightleftharpoons}} \underset{\text{product for fctfa}}{\text{acyl2}} \quad (1)$$

$$\text{product for cacsm, hacsm, macsm, macsh, cupf, ox, anmeth, dmavk}$$

(Note, for some of the reactions in reaction 1, e.g. $[Rh(sacac)(CO)(PPh_3)] + CH_3I$, the backward rate constants $k_{-1} = k_{-2} = k_{-3} = 0$. Hcacsm = methyl(2-cyclohexylamino-1-cyclopentene-1-dithiocarboxylate), Hhacsm = methyl(2-amino-1-cyclopentene-1-dithiocarboxylate), Hmacsm = methyl(2-methylamino-1-cyclopentene-1-dithiocarboxylate), Hmacsh = methyl(2-methylamino-1-cyclopentene-1-dithiocarboxylate), Hcupf = *N*-hydroxy-*N*-nitroso-benzeneamine, Hox = 8-hydroxyquinoline, Hanmeth = 4-methoxy-*N*-methylbenzothiohydroxamate, Hdmavk = dimethylaminovinylketone, Hacac = 2,4-pentanedione, Htfaa = 1,1,1-trifluoro-2,4-pentanedione, Htfdma = 1,1,1-trifluoro-5-methyl-2,4-hexanedione, Hhfaa = 1,1,1,5,5,5-hexafluoro-2,4-pentanedione, Htta = 2-thenoyltrifluoroacetone Hsacac = thioacetylacetone.)

Only two of the above mentioned studies distinguish between the reaction rates of the different isomers of $[Rh^I(L,L'\text{-BID})(CO)(PPh_3)]$ complexes containing an unsymmetrical L,L′-BID = β-diketonato ligand. For β-diketonato = tta, the final reaction product was two Rh^{III}–alkyl isomers which formed at different rates [16]. The final product for β-diketonato = fctfa, however, was two Rh^{III}–acyl isomers. The observed rate of formation or depletion of all the reaction intermediates for the oxidative addition of methyl iodide to $[Rh(fctfa)(CO)(PPh_3)]$, however, was the same [17].

Utilizing a variety spectrophotometric (UV/vis and IR) and spectroscopic (^1H and ^{31}P NMR) techniques, this paper describes the extension of this project to include the bidentate ligands $(C_4H_3S)COCHCOR^-$ with R = C_6H_5 (Ph) or C_4H_3S in an attempt to further understand the role of different bidentate ligands in the overall process taking place during the general type of reaction $[Rh^I(L,L'\text{-BID})(CO)(PPh_3)] + CH_3I$.

Reactivity of rhodium(I) dicarbonyl complexes is defined by the electron state of rhodium centre. The latter depends *inter alia* on donor–acceptor characteristics of the substituents R^1 and R^2 in the cyclic β-diketonato fragment $(R^1COCHCOR^2)^-$ of $[Rh^I(R^1COCHCOR^2)(CO)(PPh_3)]$ complexes. We were interested to establish whether a more electron donating fragment (such as C_6H_5 (Ph) or C_4H_3S) as part of a β-diketonato ligand in complexes of the type $[Rh^I((C_4H_3S)COCHCOR)(CO)(PPh_3)]$ may enhance the oxidative addition step which is the rate determining step of the Monsanto catalytic cycle. Furthermore, this study focuses on determining the nature of the final or most stable reaction product as well as the reaction rates of the different isomers of the reaction intermediates in the overall process taking place during the reaction $[Rh^I((C_4H_3S)COCHCOR)(CO)(PPh_3)] + CH_3I$ with R = C_6H_5 (Ph) or C_4H_3S.

2. Experimental

2.1. Materials and apparatus

Solid reagents used in preparations (Merck, Aldrich and Fluka) were used without further purification. Liquid reactants and solvents were distilled prior to use; water was doubly distilled. Organic solvents were dried according to published methods [19]. Melting points (m.p.) were determined with an Olympus BX51 system microscope assembled on top of a Linkam THMS600 stage and connected to a Linkam TMS94 temperature programmer.

2.2. Synthesis

The thienyl-containing β-diketones 1,3-di(2-thenoyl)-1,3-propanedione, Hdtm, and 1-phenyl-3-(2-thenoyl)-1,3-propanedione, Hbth, were prepared according to published procedures [20].

*2.2.1. [Rh(β-diketonato)(CO)$_2$] complexes **1** and **2***

The general procedure was as follow: [$Rh_2Cl_2(CO)_4$] was prepared *in situ* by refluxing $RhCl_3 \cdot 3H_2O$ (0.1 g, 0.38 mmol) in DMF (3 ml) until the colour changed from red to yellow (*ca* 30 min) [21]. The dimer-containing solution was allowed to cool on ice and an equivalent amount of solid β-diketone (0.38 mmol) was slowly added while stirring. After 30 min of stirring at room temperature, the crude product [Rh(β-diketonato)$(CO)_2$], complexes [Rh(dtm)$(CO)_2$] **1** and [Rh(bth)$(CO)_2$] **2**, was precipitated with an excess of water, filtered, air dried and recrystallized from chloroform (**1**) or hexane (**2**).

[Rh(dtm)$(CO)_2$] **1**: Yield: 0.0858 g, 57.3%. M.p. 149.2–149.9 °C. IR (cm^{-1}) = 1992 and 2057. ^{1}H NMR (δ/ppm, $CDCl_3$) 6.75 (1H, s, CH), 7.13 (2H, dd, $^3J = 5$ Hz, $^3J = 4$ Hz, CH), 7.56 (2H, dd, $^3J = 5$ Hz, $^4J = 1$ Hz, CH), 7.72 (2H, dd, $^3J = 4$ Hz, $^4J = 1$ Hz, CH). Elemental *Anal*. Calc. for $RhC_{13}H_7S_2O_4$: C, 39.6; H, 1.8. Found: C, 39.4; H, 1.6%.

[Rh(bth)$(CO)_2$] **2**: Yield: 0.1187 g, 80.5%. M.p. 147.2–148.8 °C. IR (cm^{-1}) = 1996 and 2058. ^{1}H NMR (δ/ppm, $CDCl_3$) 6.85 (1H, s, CH), 7.13 (1H, dd, $^3J = 5$ Hz, $^3J = 4$ Hz, CH), 7.47 (2H, m, CH), 7.53 (1H, m, CH), 7.58 (1H, dd, $^3J = 5$ Hz, $^4J = 1$ Hz, CH), 7.75 (1H, dd, $^3J = 4$ Hz, $^4J = 1$ Hz, CH), 7.93 (2H, m, CH). Elemental *Anal*. Calc. for $RhC_{15}H_9SO_4$: C, 46.4; H, 2.3. Found: C, 46.5; H, 2.1%.

*2.2.2. [Rh(β-diketonato)(CO)(PPh_3)] complexes **3** and **4***

The general procedure was as follow: to a solution of [Rh(β-diketonato)$(CO)_2$] (0.2 mmol) in chloroform (for **3**, warm *n*-hexane for **4**) (3 cm^3) was added a solution of PPh_3 (0.2 mmol) in chloroform (for **3**, warm *n*-hexane for **4**) (3 cm^3). The resulting reaction mixture was stirred for *ca* 1 min, until no more CO gas was released, and filtered. Pure crystals of the desired complexes [Rh(dtm)(CO)(PPh_3)] **3** and [Rh(bth)(CO)(PPh_3)] **4** were obtained.

[Rh(dtm)(CO)(PPh_3)] **3**: Yield: 0.0662 g, 52.7%. M.p. 180.0–184.5 °C. IR (cm^{-1}) = 1971. ^{1}H NMR (δ/ppm, $CDCl_3$) 6.65 (1H, s, CH), 6.89 (1H, dd, $^3J = 5$ Hz, $^3J = 4$ Hz, ring B CH), 7.08 (1H, dd, $^3J = 4$ Hz, $^4J = 1$ Hz, ring B CH), 7.11 (1H, dd, $^3J = 5$ Hz, $^3J = 4$ Hz, ring A CH), 7.27 (1H, dd, $^3J = 5$ Hz, $^4J = 1$ Hz, ring B CH), 7.41 (6H, m, CH), 7.45 (3H, m, CH), 7.52 (1H, dd, $^3J = 5$ Hz, $^4J = 1$ Hz, ring A CH), 7.73 (1 H, dd, $^3J = 4$ Hz, $^4J = 1$ Hz, ring A CH), 7.74 (6 H, m, CH). Elemental *Anal*. Calc. for $RhC_{30}PH_{22}S_2O_3$: C, 57.3; H, 3.5. Found: C, 57.0; H, 3.2%.

[Rh(bth)(CO)(PPh_3)] **4**: Yield: 0.0830 g, 66.7%. M.p. 149.1–189.5 °C. IR (cm^{-1}) = 1970. ^{1}H NMR (δ/ppm, $CDCl_3$) 6.74 (1H, s, isomer A CH), 6.75 (1H, s, isomer B CH), 6.89 (1H, dd, $^3J = 5$ Hz, $^3J = 4$ Hz, isomer A CH), 7.10 (3H, m, isomer B CH), 7.10 (1H, dd, $^3J = 4$ Hz, $^4J = 1$ Hz, isomer A CH), 7.11 (1 H, dd, $^3J = 5$ Hz, $^3J = 4$ Hz, isomer B CH), 7.27 (1H, dd, $^3J = 5$ Hz, $^4J = 1$ Hz, isomer A CH), 7.42 (14H, m, CH), 7.47 (9H, m, CH), 7.52 (1H, dd, $^3J = 5$ Hz, $^4J = 1$ Hz, isomer B CH), 7.75 (12 H, m, CH), 7.76 (1H, dd, $^3J = 4$ Hz, $^4J = 1$ Hz, isomer B CH), 8.01 (2H, m, isomer A CH). Elemental *Anal*. Calc. for $RhC_{32}PH_{24}SO_3$: C, 61.7; H, 3.9. Found: C, 61.5; H, 3.7%.

2.3. Spectroscopy and spectrophotometry

NMR measurements at 298 K were recorded on a Bruker Advance DPX 300 NMR spectrometer [^{1}H (300.130 MHz)] and a Bruker Advance II 600 NMR spectrometer [^{1}H (600.130 MHz) and ^{31}P (242.937 MHz)]. The chemical shifts were reported relative to $SiMe_4$ (0.00 ppm) for the ^{1}H spectra, and relative to 85% H_3PO_4 (0 ppm) for the ^{31}P spectra. Positive values indicate downfield shift. IR spectra were recorded from neat samples on a Digilab FTS 2000 infrared spectrophotometer utilizing a He–Ne laser at 632.6 nm. UV/vis spectra were recorded on a Cary 50 Probe UV/vis spectrophotometer.

2.4. Kinetic measurements

Oxidative addition reactions were monitored on the IR (by monitoring formation and disappearance of the carbonyl peaks), on the UV/vis (by monitoring the change in absorbance at the indicated wavelength) spectrophotometers and on the NMR (by monitoring the change in integration units of the specified signals) spectrometer. All kinetic measurements were monitored under pseudo-first-order conditions with [CH_3I] 10–5000 times the concentration of the [Rh^I(β-diketonato)(CO)(PPh_3)] complex in the specified solution. The concentration [Rh^I(β-diketonato)(CO)(PPh_3)] $\cong 0.00005$ mol dm^{-3} for UV/vis measurements, $\cong 0.008$ mol dm^{-3} for IR measurements and $\cong 0.014$ mol dm^{-3} for NMR measurements. Kinetic measurements under pseudo-first-order conditions for different concentrations of [Rh^I(β-diketonato)(CO)(PPh_3)] at a constant [CH_3I], confirmed that the concentration of [Rh^I(β-diketonato)(CO)(PPh_3)] did not influence the value of the observed kinetic rate constant. The observed first-order rate constants were obtained from least-squares fits of absorbance (IR and UV/vis) or integration units (NMR) versus time data [22].

The [Rh^I(β-diketonato)(CO)(PPh_3)] complexes **3** and **4** were tested for stability in chloroform by means of overlay IR and UV/vis spectra for at least 24 h. A ^{1}H NMR spectrum of the title compound after 48 h in solution of $CDCl_3$ confirmed stability in solution. A linear relationship between UV/vis absorbance (A) and concentration (c) confirms the validity of the Beer Lambert law ($A = \varepsilon c l$ with l = path length = 1 cm) for **3** and **4**.

2.5. Calculations

Pseudo-first-order rate constants, k_{obs}, were calculated by fitting [22] kinetic data to the first-order equation [23]

$$[A]_t = [A]_0 e^{(-k_{obs}t)} \quad (2)$$

with $[A]_t$ and $[A]_0$ the absorbance of the indicated species at time t and at $t = 0$ (UV/vis or IR experiments) or integral values for the specified peaks on NMR spectra. The experimentally determined pseudo-first-order rate constants were converted to second order rate constants, k_1, by determining the slope of the linear plots of k_{obs} against the concentration of the incoming CH_3I ligand. Non-zero intercepts implied that

$$k_{obs} = k_1[CH_3I] + k_{-1} \quad (3)$$

and that the k_{-1} step in the proposed reaction mechanism exists.

The activation parameters $\Delta H^{\#}$ (activation enthalpy) and $\Delta S^{\#}$ (activation entropy), for the oxidative addition reactions were determined from least-squares fits [22] of the reaction rate constants versus temperature data according to the Eyring relationship, [24] in the linear form

$$\ln\frac{k}{T} = -\frac{\Delta H^{\#}}{RT} + \frac{\Delta S^{\#}}{R} + \ln\frac{k_B}{h} \quad (4)$$

with k = rate constant, k_B = Boltzmann's constant, T = temperature, h = Planck's and R = universal gas constant. The activation free energy $\Delta G^{\#} = \Delta H^{\#} - T\Delta S^{\#}$.

All kinetic mathematical fits were done utilizing the fitting program MINSQ [22]. The error of all the data is presented according to crystallographic conventions. For example $k_{obs} = 0.0236(1)\ s^{-1}$ implies $k_{obs} = (0.0236 \pm 0.0001)\ s^{-1}$.

3. Results and discussion

3.1. Synthesis and identification of complexes

The route utilized to obtain the new dicarbonyl rhodium(I) complexes of general formula [Rh((C$_4$H$_3$S)COCHCOR)(CO)$_2$] is given in Scheme 1. The new brick-red [Rh(β-diketonato)(CO)(PPh$_3$)] complexes **3** and **4** with β-diketonato = dtm (**3**) and bth (**4**) respectively were obtained by reacting an equivalent amount of PPh_3 with [Rh(β-diketonato)(CO)$_2$] in a chloroform medium (for **3**, warm *n*-hexane for **4**). The [Rh(β-diketonato)(CO)(PPh$_3$)] product immediately precipitates out. The thenoyl-containing rhodium complexes **1**–**4** are all acid sensitive and decompose on silicagel. NMR studies therefore had to be performed in $CDCl_3$ which was passed through basic alumina prior use. ^{1}H NMR spectra show that, for the [Rh(bth)(CO)(PPh$_3$)] **4**, two isomers exist in solution. Regarding the two possible isomers of **4**, we chose to label the isomer with CO *trans* to the oxygen atom nearest to the more electron donating thienyl group of the β-diketonato chelate ring as isomer A, while the other isomer is labelled isomer B (Scheme 1). Focussing on the positions of the signals of the ^{1}H NMR spectrum of the thienyl group of [Rh(bth)(CO)(PPh$_3$)] **4**, the set of signals belonging to an isomer in the more upfield position, due to the shielding effect through space of the PPh_3 group, is assigned to isomer B. The position of the thienyl resonances of the two isomers was confirmed by two dimensional ^{1}H–^{1}H TOCSY. The equilibrium constant, defined as K_c = [isomer B]/[isomer A] and applicable to the equilibrium shown in Scheme 1, may be determined by calculating the ratio of peak integral values of non-overlapping corresponding signals of each isomer and averaging all answers giving $K_{c1} = 1.0$ in $CDCl_3$ or $K_{c1} = 0.8$ in acetone-d_6 for **4**. The time required for the two isomers of **4** to reach the solution equilibrium position, according to Scheme 1, was shorter than the time required to dissolve the complex and to record data for a NMR spectrum.

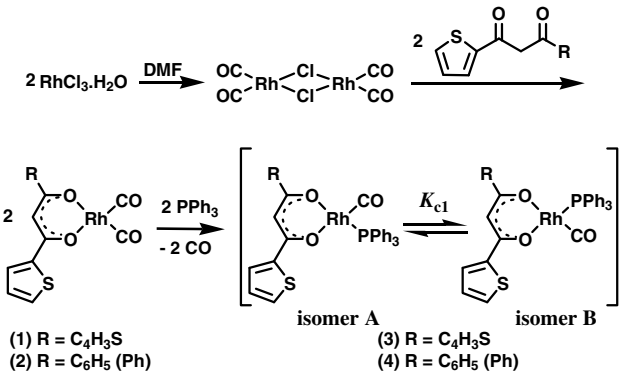

Scheme 1. Synthetic routes for the synthesis of the [Rh^I(β-diketonato)(CO)$_2$] complexes **1** and **2** and [Rh^I(β-diketonato)(CO)(PPh$_3$)] complexes **3** and **4** from $RhCl_3 \cdot 3H_2O$.

3.2. Kinetics

3.2.1. Infrared study

Kinetic measurements for the reaction of [Rh(dtm)(CO)(PPh$_3$)] **3** or [Rh(bth)(CO)(PPh$_3$)] **4** with methyl iodide in $CHCl_3$ were first carried out using IR spectroscopy by monitoring the changes in absorbance of peaks at different ν(CO) bands. This technique is ideal to distinguish between CO bonds in metal–CO complexes that resonate at ~1980–2000 cm^{-1} for Rh^I–carbonyl complexes, at ~2050–2100 cm^{-1} for Rh^{III}–carbonyl complexes and CO bonds in metal–$COCH_3$ complexes that resonates at ~1700–1750 cm^{-1} for Rh^{III}–acyl complexes [25]. A typical series of the spectra of the oxidative addition reaction of CH_3I to **3** or to **4**, as well as the subsequent carbonyl insertion and deinsertion steps, are shown in Fig. 1. The first reaction step for **3** indicates the disappearance of the ν(CO) band of the rhodium(I) reactant at 1987 cm^{-1} and the simultaneous appearance of two new ν(CO) bands at 2079 cm^{-1} and 1720 cm^{-1} exactly at the same rate as the

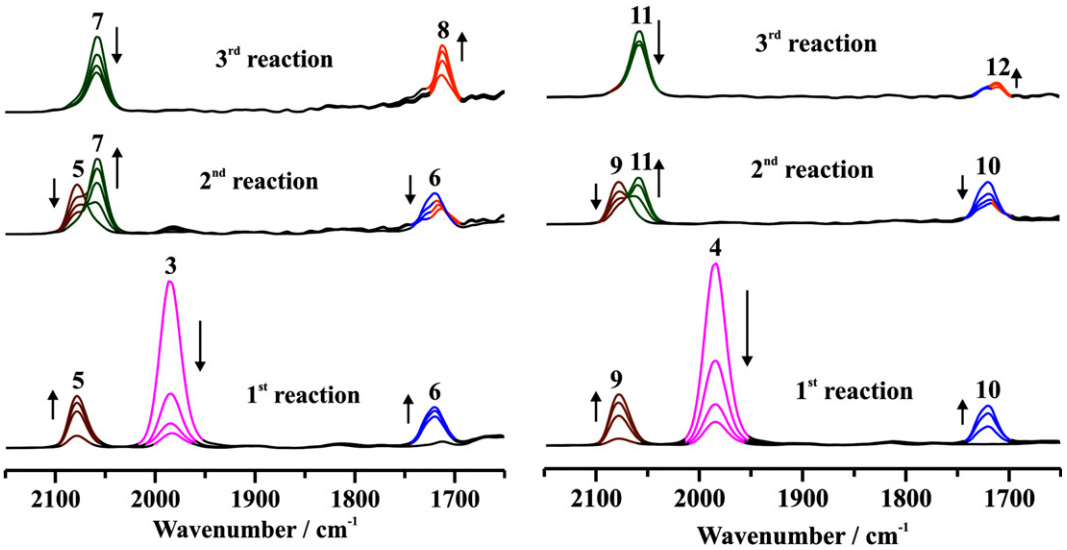

Fig. 1. Illustration of the oxidative addition reaction between CH_3I and [Rh(dtm)(CO)(PPh_3)] **3** (left) and [Rh(bth)(CO)(PPh_3)] **4** (right) as monitored on the IR spectrophotometer between 1650 and 2150 cm^{-1} in chloroform at 25 °C. Both complexes follow the same reaction sequence. The *first reaction* is indicated by the disappearance of Rh^I and the simultaneous appearance of Rh^{III}–alkyl1 and Rh^{III}–acyl1, all at the same rate. The *second reaction* is indicated by the simultaneous disappearance of Rh^{III}–alkyl1 and Rh^{III}–acyl1 and the formation of a Rh^{III}–alkyl2 species. The *third reaction* is indicated by the disappearance of Rh^{III}–alkyl2 and the formation of a Rh^{III}–acyl2 species. The numbering of the different intermediates is as indicated in Table 1. The *y*-axis represents relative absorbance.

disappearance of **3**. The band at 2079 cm^{-1} is assigned to a Rh^{III}–alkyl product [Rh(dtm)(CH_3)(CO)(PPh_3)(I)] **5** and the band at 1720 cm^{-1} to a Rh^{III}–acyl product [Rh(dtm)($COCH_3$)(PPh_3)(I)] **6**. These first Rh^{III}–alkyl and Rh^{III}–acyl products that form will be labelled Rh^{III}–alkyl1 and Rh^{III}–acyl1 for further indication. The Rh^{III}–acyl1 results from the migration insertion of the methyl group of the Rh^{III}–alkyl1 to the carbonyl group. The exponential decay observed for the reactant *v*(CO) band for **3** showed the reaction to be first order in [rhodium(I)]. The second order rate constants, k_1, for the oxidative addition reaction of CH_3I to both **3** and **4**, are given in Table 2.

The result that the Rh^{III}–alkyl1 **5** species forms at *exactly* the same rate as the Rh^{III}–acyl1 **6** species, is considered to imply that an equilibrium exists between the Rh^{III}–alkyl1 **5** and Rh^{III}–acyl1 **6** that is fast enough to be maintained on the timescale of [Rh(dtm)(CO)(PPh_3)] **3** disappearance [16]. The *first reaction* that can thus be presented as follow:

$$Rh^I + CH_3I \underset{k_{-1}}{\overset{K_1, k_1}{\rightleftharpoons}} \left\{[Rh^{III}\text{-alkyl1}] \underset{k_{-2}}{\overset{K_2, k_2}{\rightleftharpoons}} [Rh^{III}\text{-acyl1}]\right\} \quad (5)$$

A *second* much slower ($t_{1/2} \approx 6$ h) *reaction*, as observed on the IR, is also illustrated in Fig. 1. The reaction products of the reaction between **3** and CH_3I, the Rh^{III}–alkyl1 **5** at 2079 cm^{-1} and the Rh^{III}–acyl1 **6** at 1720 cm^{-1} disappear at the same rate ($k_{obs} = 0.000033(1)\ s^{-1}$) as the formation of a second alkyl product, Rh^{III}–alkyl2, **7** ($k_{obs} = 0.000034(1)\ s^{-1}$), at another *v*(CO) = 2056 cm^{-1}. By comparing the rate constants, the *second reaction* is 0.0026/0.000034 ≈75 times slower than the *first reaction* for $[CH_3I] = 0.1$ mol dm^{-3}. Further evidence that there exists a *fast* equilibrium between the Rh^{III}–alkyl1 and Rh^{III}–acyl1 products are found from the observation that the Rh^{III}–alkyl1 **5** at 2079 cm^{-1} disappears at the same rate as the Rh^{III}–acyl1 **6** at 1720 cm^{-1}. Since the *second reaction* is much slower than the *first reaction*, it was treated in isolation. Data from the interface at the boundary between the two reactions were, however, disregarded. This *second reaction* was found to be independent of $[CH_3I]$. The kinetic data of the *second reaction* are consistent with:

$$\left\{[Rh^{III}\text{-alkyl1}] \underset{k_{-2}}{\overset{2, k_2}{\rightleftharpoons}} [Rh^{III}\text{-acyl1}]\right\} \underset{k_{-3}}{\overset{k_3}{\rightleftharpoons}} [Rh^{III}\text{-alkyl2}] \quad (6)$$

The *second reaction* was followed by a very slow ($t_{1/2} \approx 2$ days) *third reaction*. This *third reaction*, also illustrated in Fig. 1, includes the slow first-order disappearance of the Rh^{III}–alkyl2 **7** ($k_{obs} = 0.0000036(3)\ s^{-1}$) at 2056 cm^{-1} and the appearance, at the same rate, of a new acyl product, Rh^{III}–acyl2 **8** at 1713 cm^{-1} ($k_{obs} = 0.0000044(2)\ s^{-1}$). These two rates are within experimental error identical (average = 0.0000040 s^{-1}). Both are independent of $[CH_3I]$. The long half-life of the *third reaction* implied that it could not be followed with great accuracy, as solvent evaporation became difficult to control. The kinetic data of the *third reaction* are consistent with:

$$[Rh^{III}\text{-alkyl2}] \underset{k_{-4}}{\overset{k_4}{\rightleftharpoons}} [Rh^{III}\text{-acyl2}] \quad (7)$$

The overall reaction sequence for this oxidative addition reaction may therefore be represented as

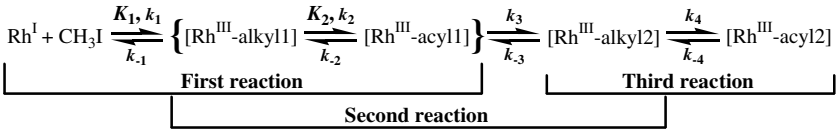

(8)

The same reaction pattern (Eq. (8)) was observed on the IR for the oxidative addition reaction of CH_3I to [Rh(bth)(CO)(PPh_3)] **4** (Fig. 1). Though, the third reaction, that involves the formation of a second acyl species, observed for both **3** and **4**, was not observed for the oxidative addition and the following carbonyl insertion and deinsertion of $[Rh^I((C_4H_3S)COCHCOCF_3)(CO)(PPh_3)] + CH_3I$ [16].

It was possible, due to the long half-life of the *second reaction*, to isolate the [Rh(dtm)(CO)(PPh_3)]–alkyl2 **7** and the [Rh(bth)(CO)(PPh_3)]–alkyl2 **11** from the reaction mixture before the formation of the Rh^{III}–acyl2 species. The spectroscopic data of **7** and **11** are included in Table 1. Complexes **7** and **11** were stable in the solid state, but in solution and in the presence of an excess CH_3I, CO insertion occurred at a slow rate to form the Rh^{III}–acyl2 product.

3.2.2. UVlvis study

The reaction between CH_3I and [Rh(dtm)(CO)(PPh_3)] **3** and the reaction between CH_3I and [Rh(bth)(CO)(PPh_3)] **4** were also monitored on an UV/vis spectrophotometer and all three reaction steps could be identified for both reactants (Fig. 2). The reaction rate constant obtained for the first step corresponded to the rate constant for the disappearance of the Rh^I monocarbonyl species as observed by IR. The rate constant for the second and third steps also corresponded to the rate constant for the *second* and *third reactions* as observed on the IR spectrophotometer. The second step is the formation of the Rh^{III}–alkyl2 species and the third step is the formation of the final reaction product, the Rh^{III}–acyl2 species.

In chloroform, the *first*, *second* and *third reactions* were best followed at 440, 380 and 450 respectively for **3** and at 430, 380 and 395 nm respectively for **4**. All three the reaction steps of **3** and **4** could be followed at 450 and 395 nm respectively, giving rate constants in agreement with those obtained at other wavelengths (Fig. 2).

Plots of k_{obs} for the *first reaction* of both **3** and **4** versus $[CH_3I]$ are linear (Fig. 3), indicating the reaction to be first order in CH_3I and hence second order overall. Second order rate constants, k_1 in reaction 8, and activation parameters (Eyring plots insets in Fig. 3) are listed in Table 2.

Table 1
^1H, ^{31}P NMR and IR spectral parameters of the [Rh^I(β-diketonato)(CO)(PPh_3)], Rh^{III}(β-diketonato)(CH_3)(CO)(PPh_3)(I)] and [Rh^{III}(β-diketonato)($COCH_3$)(PPh_3)(I)] complexes (β-diketonato = bth or dtm)

No.	Compound	^{31}P NMR		^1H NMR					IR
		$\delta^{31}P$/ppm	$^1J(^{31}P–^{103}Rh)$/Hz	δ^1H methine proton β-diketonato ligand/ppm	Methyl protons from CH_3I			K_c	ν_{CO}/cm^{-1}
					δ^1H/ppm	$^2J(^1H–^{13}C–^{103}Rh)$/Hz	$^3J(^1H–^{13}C–^{103}Rh–^{31}P)$/Hz		
β-diketonato = dtm									
3	Rh^I	47.61	176	6.65					1987
5	Rh^{III}–alkyl1	31.22	126	6.74	1.60	1.5	2.2	–	2079
6	Rh^{III}–acyl1	37.16	154	6.68	3.03				1720
7	Rh^{III}–alkyl2	28.93	117	6.03	1.83	1.8	3.8		2056
8	Rh^{III}–acyl2	35.5	159	[a]	3.05				1713
β-diketonato = bth									
4A	Rh^I–A	47.41	176	6.74				1.0	1983
4B	Rh^I–B	49.21	177	6.75					
9A	Rh^{III}–alkyl1A	31.03	128	6.67	1.59	1.7	2.2	0.4	2079
9B	Rh^{III}–alkyl1B	34.21	128	6.78	1.60	1.7	2.2		
10A	Rh^{III}–acyl1A	38.50	154	6.80	3.02			0.8	1720
10B	Rh^{III}–acyl1B	36.89	154	6.83	3.09				
11A	Rh^{III}–alkyl2A	28.62	121	6.10	1.85	2.0	3.8	1.4	2056
11B	Rh^{III}–alkyl2B	29.21	121	6.09	1.85	2.0	3.8		
12A	Rh^{III}–acyl2A	35.16	156	[a]	3.00				1709
12B	Rh^{III}–acyl2B	35.81	160	[a]	3.04				

K_c = [isomer-B]/[isomer-A] at equilibrium at 25 °.
[a] Not determined due to overlapping of peaks.

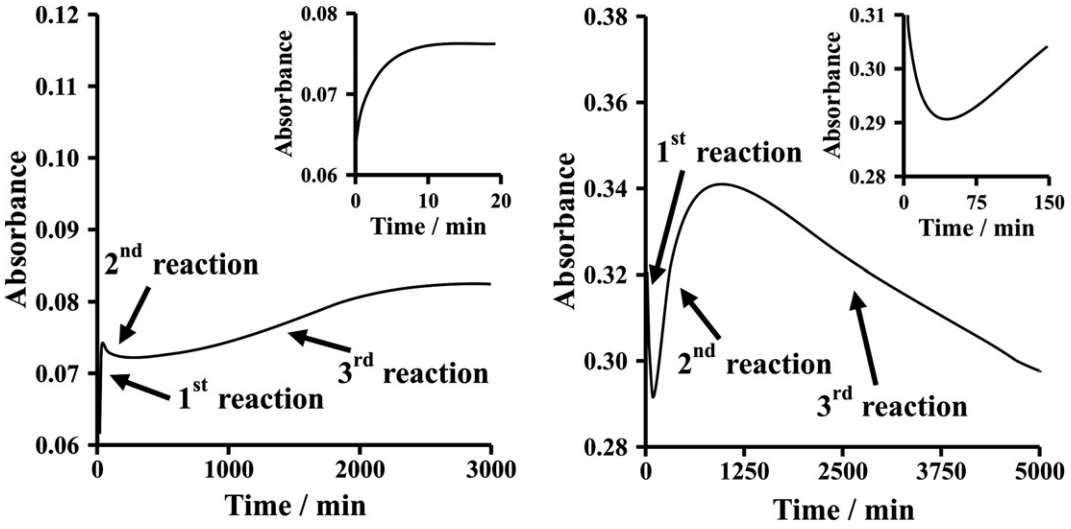

Fig. 2. Absorbance vs. time data at 25 °C for the UV/vis monitored oxidative addition reaction and alkyl and acyl interconversions for the reaction between CH_3I and [Rh(dtm)(CO)(PPh_3)] **3** (left) and [Rh(bth)(CO)(PPh_3)] **4** (right) in chloroform at 450 and 395 nm respectively, illustrating the three reactions observed for both complexes. The insets give enlargements of the first reaction.

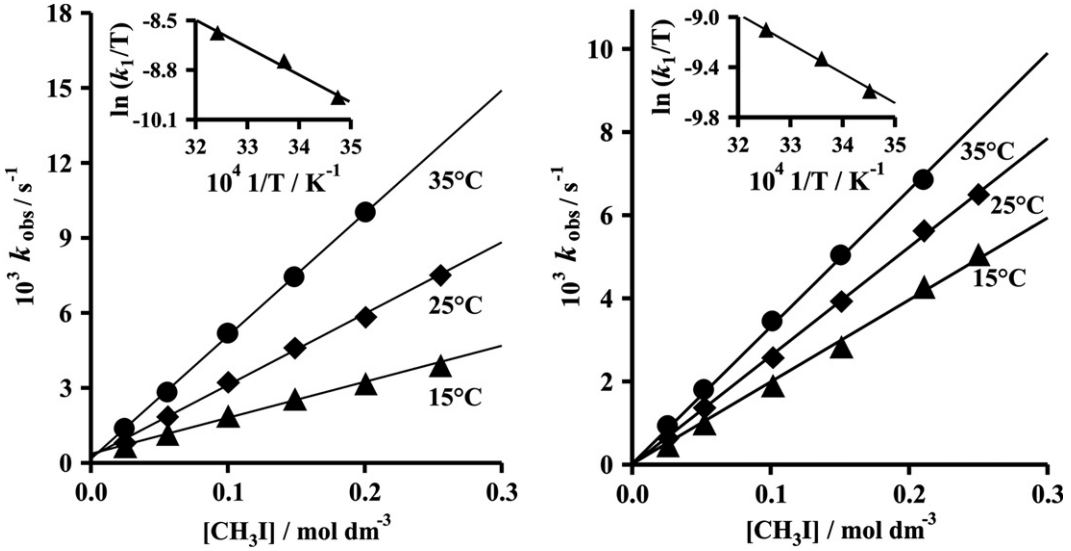

Fig. 3. Temperature and CH_3I concentration dependence of the oxidative addition of CH_3I to [Rh(dtm)(CO)(PPh_3)] **3** (left) and [Rh(bth)(CO)(PPh_3)] **4** (right), as monitored on the UV/vis spectrophotometer in chloroform, for the *first reaction* {$Rh^I + CH_3I \rightleftharpoons [Rh^{III}$–alkyl1 $\rightleftharpoons Rh^{III}$–acyl1]}. Inset: Linear dependence between $\ln(k_1/T)$ and $1/T$ as predicted by the Eyring equation.

Incorporation of a more electron donating fragment (such as C_6H_5 or C_4H_3S) in the β-diketonato ligand $(C_4H_3S)COCHCOR^-$ thus significantly enhances the rate of the oxidative addition step (first reaction step) of the reaction $[Rh^I((C_4H_3S)COCHCOR)(CO)(PPh_3)] + CH_3I$ when compared to the rate of oxidative addition step of the corresponding $(C_4H_3S)COCHCOCF_3^-$ complex containing the electron withdrawing CF_3 group in the cyclic β-diketonato fragment: k_1 ($dm^3\,mol^{-1}\,s^{-1}$) = 0.022(6) (R = C_4H_3S), 0.026(3) (R = C_6H_5) and 0.00171(4) (R = CF_3).

3.2.3. ^1H and ^{31}P NMR study

The reaction between CH_3I and **3** and between CH_3I and **4** were also monitored by ^1H and ^{31}P NMR in order to obtain additional insight into this reaction. NMR spectroscopy is an excellent technique for the identification of the different isomers resulting from the oxidative addition reaction of [Rh^I(β-diketonato)(CO)-(PPh_3)] with methyl iodide. By carefully comparing the positions and integrals of the different signals, the spectral parameters of the different reaction products during the oxidative addition reaction and subsequent carbonyl insertion and deinsertion reactions, could be identified (Table 1). The same reaction sequence, as observed on IR and UV/vis, was observed on ^1H NMR (Fig. 4) and ^{31}P NMR (Fig. 5). The new feature introduced by the NMR study is the existence of more than one isomer for each intermediate of the reaction products of the two

Table 2
The kinetic rate constants of the oxidative addition reaction between CH_3I and [Rh(β-diketonato)(CO)(PPh_3)] as obtained by various spectrophotometric and spectroscopic methods in chloroform at 25 °C for β-diketonato = bth, dtm and tta

Method	k_1/dm^3 mol^{-1} s^{-1}	k_{-1}/s^{-1}	k_3/s^{-1}	k_4/s^{-1}	$\Delta H^{\#}(k_1)$/kJ mol^{-1}	$\Delta S^{\#}(k_1)$/J mol^{-1} K^{-1}	$\Delta G^{\#}(k_1)$/kJ mol^{-1}
[Rh(dtm)(CO)(PPh_3)] **3**							
IR	0.026(3)	0.0003(2)	0.000032(6)	0.000004(1)			
UV/vis	0.029(1)	0.0002(2)	0.0000349(5)	0.000005(1)	40(6)	−130(20)	80(3)
^{1}H NMR	0.0296(2)		0.000030(2)	0.000004(1)			
^{1}31P NMR	0.023(2)		0.000030(5)	[a]			
[Rh(bth)(CO)(PPh_3)] **4**							
IR	0.022(6)	0.0000(2)	0.000029(9)	[a]			
UV/vis	0.0265(6)	0.0000(1)	0.000059(3)	0.000003(2)	16.8(8)	−218(3)	82(2)
^{1}1H NMR[b]	0.028(3)		0.000049(5)	[a]			
^{1}31P NMR[b]	0.0226(9)		0.000029(6)	[a]			
[Rh(tta)(CO)(PPh_3)] [16]							
UV/vis	0.00171(4)	0.000023(6)	0.0005(1)	[c]	31.1(5)	−194(2)	89(1)

k_1, k_3 and k_4 are the rate constants associated with the *first, second* and *third stages* of the reaction of CH_3I to [Rh(β-diketonato)(CO)(PPh_3)].
[a] The disappearance of the Rh^{III}–alkyl2 and the appearance of the Rh^{III}–acyl2 were observed, but due to the long half-life (~2 days) of the *third reaction*, the kinetics could not be followed with accuracy.
[b] Two isomers observed for each product. The observed rate constants for each isomer were the same within experimental error.
[c] No third reaction step observed.

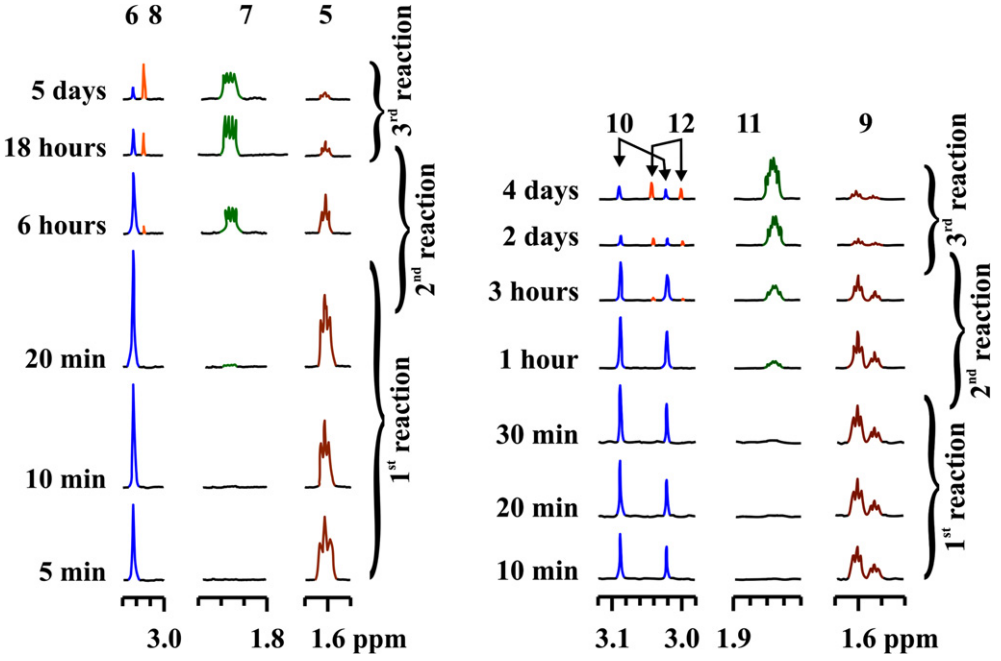

Fig. 4. Fragments of the methyl region of the ^{1}H NMR spectra in $CDCl_3$ illustrating the reaction sequence during the oxidative addition and the following carbonyl insertion and deinsertion reactions of 0.0268 mol dm^{-3} [Rh(dtm)(CO)(PPh_3)] **3** reacting with 0.150 mol dm^{-3} CH_3I (left) and 0.0262 mol dm^{-3} [Rh(bth)(CO)(PPh_3)] **4** reacting with 0.159 mol dm^{-3} CH_3I (right) in $CDCl_3$ ($T = 25$ °C) at the indicated time intervals. Note that two isomers for each species can be observed for **4** which contain an unsymmetrical β-diketonato ligand, while only one isomer for each reaction intermediate can be observed for **3** which contain a symmetrical β-diketonato ligand. The *first reaction* is illustrated by the growing signals of the CH_3-group of indicated Rh^{III}–acyl1 isomers at *ca.* 3 ppm and of Rh^{III}–alkyl1 isomers at *ca.* 1.5 ppm. The *second reaction* is illustrated by the decrease of the various signals representing Rh^{III}–alkyl1 and Rh^{III}–acyl1 species with the simultaneous increase in the signals of the CH_3-group of the Rh^{III}–alkyl2 spesies at *ca.* 1.9 ppm. The *third reaction* is illustrated by the change in signal intensity of the CH_3-group of the Rh^{III}–alkyl2 isomers at *ca.* 1.9 ppm and the appearance of a new Rh^{III}–acyl2 species at *ca.* 3.0 ppm. The multiplet of the CH_3 group of the Rh^{III}–alkyl1 and Rh^{III}–alkyl2 isomers is due to coupling with Rh (spin 1/2) and P (spin 1/2). The numbering of the different isomers is as indicated in Table 1.

isomers of [Rh((C$_4$H$_3$S)COCHCO(C$_6$H$_5$))(CO)(PPh_3)] **4** with methyl iodide. Only one isomer of each intermediate was observed for the reaction products of [Rh((C$_4$H$_3$S)COCHCO(C$_4$H$_3$S))(CO)(PPh_3)] **3**, since this complex contains a symmetrical β-diketonato ligand (C$_4$H$_3$S)COCHCO(C$_4$H$_3$S)$^-$.

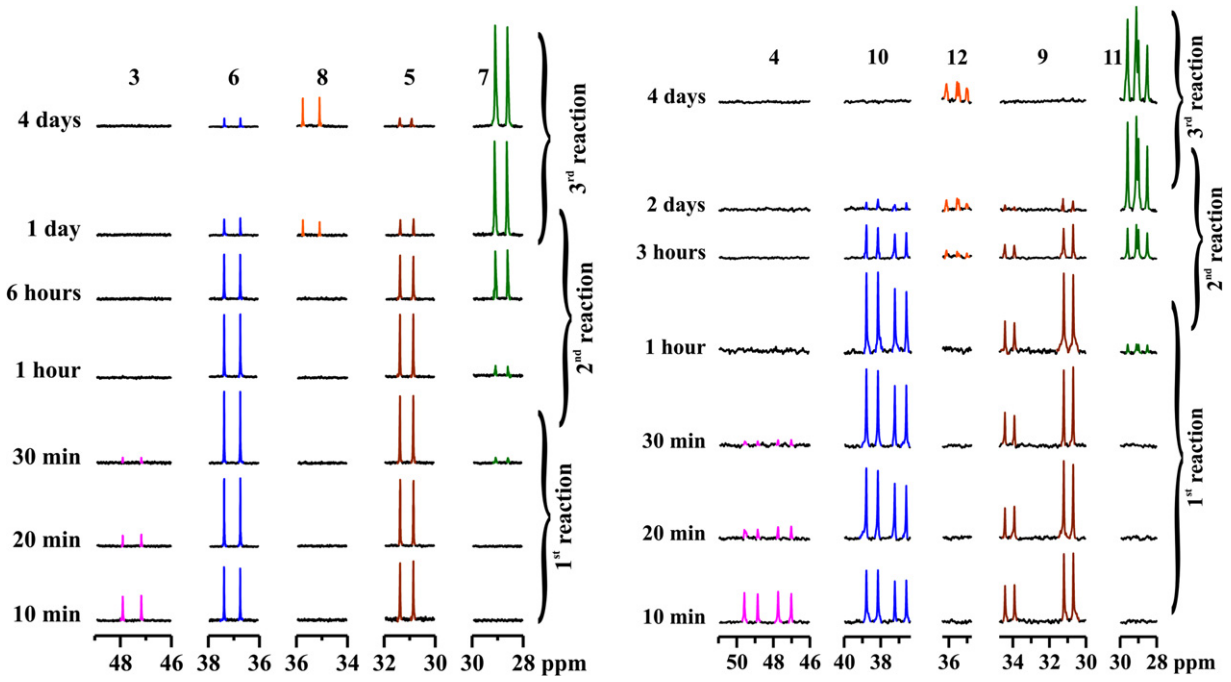

Fig. 5. Selected ^{31}P NMR spectra illustrating doublet ^{31}P peaks of the indicated reactants and products during the three reactions for the oxidative addition of CH_3I to [Rh(dtm)(CO)(PPh_3)] **3** (left) and [Rh(bth)(CO)(PPh_3)] **4** (right) in $CDCl_3$ ($T = 25$ °C) at the indicated time intervals. Note that two isomers for each species can be observed for **4** (which contain an unsymmetrical β-diketonato ligand), while only one isomer for each reaction intermediate can be observed for **3** (which contain a symmetrical β-diketonato ligand). The doublet of each signal is due to coupling with Rh (spin 1/2). The numbering of the different isomers is as indicated in Table 1.

The two observed isomers of each intermediate in the reaction of **4** will be referred to as A and B, see Table 1. The choice of the labels is arbitrary and has no significance. NMR kinetic results indicate that the A and B isomer of each species exists in a fast equilibrium with each other, since the observed rate constant for the depletion or formation of an A and a B isomer of the same species was found to be, within experimental error, the same. Furthermore, the ratio Rh^I–B/Rh^I-A = 1.0 (obtained by integral evaluation) is not the same as the ratio Rh^{III}–alkyl1B/Rh^{III}–alkyl1A = 0.40 or the ratio Rh^{III}–acyl1B/Rh^{III}–acyl1A = 0.8, etc. (Table 1). If the reaction was

$$\mathrm{Rh^I\text{-}A} + \mathrm{CH_3I} \underset{k_{-1}}{\overset{K_1, k_1}{\rightleftharpoons}} \{[\mathrm{Rh^{III}\text{-}alkyl1A}] \underset{k_{-2}}{\overset{K_2, k_2}{\rightleftharpoons}} [\mathrm{Rh^{III}\text{-}acyl1A}]\} \underset{k_{-3}}{\overset{k_3}{\rightleftharpoons}} [\mathrm{Rh^{III}\text{-}alkyl2A}] \underset{k_{-4}}{\overset{k_4}{\rightleftharpoons}} [\mathrm{Rh^{III}\text{-}acyl2A}] \quad (9)$$

for the A isomers and separately

$$\mathrm{Rh^I\text{-}B} + \mathrm{CH_3I} \underset{k_{-1}}{\overset{K_1, k_1}{\rightleftharpoons}} \{[\mathrm{Rh^{III}\text{-}alkyl1B}] \underset{k_{-2}}{\overset{K_2, k_2}{\rightleftharpoons}} [\mathrm{Rh^{III}\text{-}acyl1B}]\} \underset{k_{-3}}{\overset{k_3}{\rightleftharpoons}} [\mathrm{Rh^{III}\text{-}alkyl2B}] \underset{k_{-4}}{\overset{k_4}{\rightleftharpoons}} [\mathrm{Rh^{III}\text{-}acyl2B}] \quad (10)$$

for the B isomers, and if no equilibrium between isomers A and B existed, the ratio B:A of these isomers would have been the same throughout the entire reaction sequence involving three different steps.

Taking into account that two main isomers exist of each reactant and reaction product of **4**, the complete reaction sequence for the oxidative addition of CH_3I to **4** containing an unsymmetrical β-diketonato ligand, is therefore as given in reaction (11)

$$\underbrace{\underbrace{\begin{bmatrix} \mathrm{Rh^I\text{-}A} \\ \rightleftharpoons K_{c1} \\ \mathrm{Rh^I\text{-}B} \end{bmatrix} + \mathrm{CH_3I} \overset{K_1, k_1}{\underset{k_{-1}}{\rightleftharpoons}} \begin{bmatrix} [\mathrm{Rh^{III}\text{-}alkyl1A}] \\ \rightleftharpoons K_{c2} \\ [\mathrm{Rh^{III}\text{-}alkyl1B}] \end{bmatrix} \overset{K_2, k_2}{\underset{k_{-2}}{\rightleftharpoons}} \begin{bmatrix} [\mathrm{Rh^{III}\text{-}acyl1A}] \\ \rightleftharpoons K_{c3} \\ [\mathrm{Rh^{III}\text{-}acyl1B}] \end{bmatrix}}_{\text{First reaction}} \overset{k_3}{\underset{k_{-3}}{\rightleftharpoons}} \underbrace{\begin{bmatrix} [\mathrm{Rh^{III}\text{-}alkyl2A}] \\ \rightleftharpoons K_{c4} \\ [\mathrm{Rh^{III}\text{-}alkyl2B}] \end{bmatrix} \overset{k_4}{\underset{k_{-4}}{\rightleftharpoons}} \begin{bmatrix} [\mathrm{Rh^{III}\text{-}acyl2A}] \\ \rightleftharpoons K_{c5} \\ [\mathrm{Rh^{III}\text{-}acyl2B}] \end{bmatrix}}_{\text{Third reaction}}}_{\text{Second reaction}} \quad (11)$$

and for the symmetrical β-diketonato ligand **3** as given in reaction 8.

The above reaction sequence where the observed rate of formation of the two [Rh((C$_4$H$_3$S)COCHCOR)(CH$_3$)-(CO)(PPh$_3$)(I)]–alkyl2 isomers, R = C$_6$H$_5$, is the same due to the fast equilibrium K_{c4}, is contrary to what was found

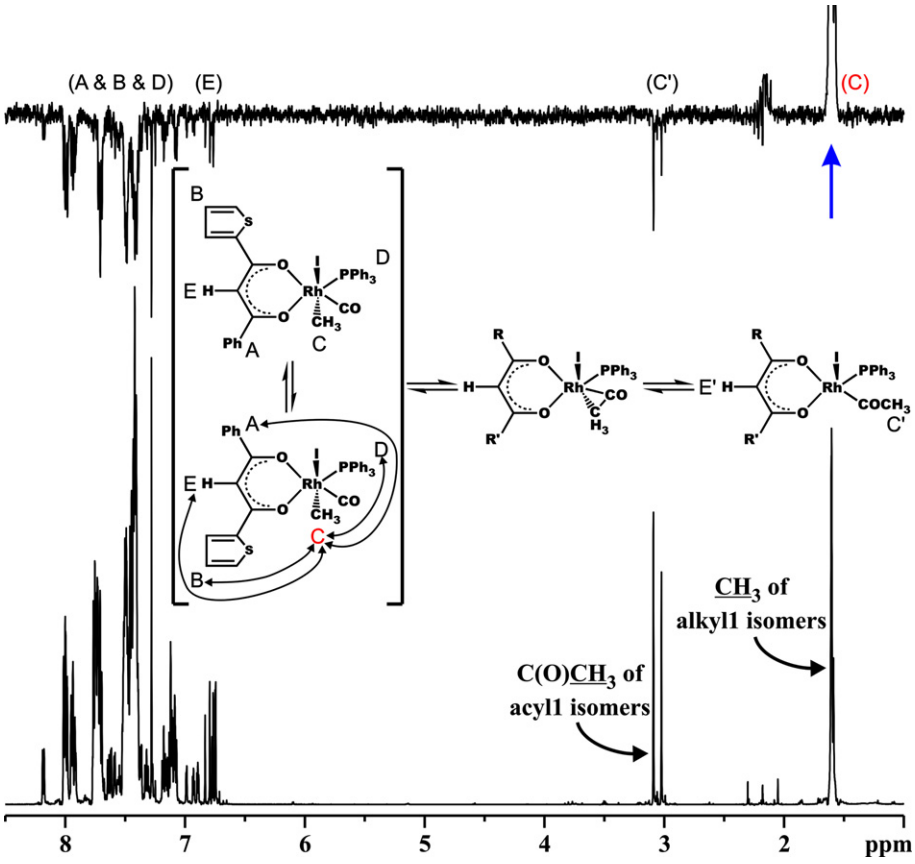

Fig. 6. ^{1}H NMR spectrum (bottom) of a reaction mixture containing the [Rh(bth)(CH_3)(CO)(PPh_3)(I)]–alkyl1 isomers and the [Rh(bth)($COCH_3$)(PPh_3)(I)]–acyl1 isomers in a fast equilibrium with each other. At the top is the ^{1}H–^{1}H NOESY observed when irradiating on the methyl group of the two [Rh(bth)(CH_3)(CO)(PPh_3)(I)]–alkyl1 isomers at 1.6 ppm. The peaks observed at 3 ppm are a result of the fast equilibrium [Rh(bth)(CH_3)(CO)(PPh_3)(I)]–alkyl1 ⇌ [Rh(bth)($COCH_3$)(PPh_3)(I)]–acyl1. CH_3I peak is suppressed for clarity.

for the oxidative addition of CH_3I to [Rh((C_4H_3S)COCHCOR)(CO)(PPh_3)], with R = CF_3, where the [Rh((C_4H_3S)COCHCOCF_3)(CH_3)(CO)(PPh_3)(I)]–alkyl2A isomer formed at a different rate than the [Rh((C_4H_3S)COCHCOCF_3)(CH_3)(CO)(PPh_3)(I)]–alkyl2B isomer (no [Rh((C_4H_3S)COCHCOCF_3)($COCH_3$)(PPh_3)(I)]–acyl2 isomers were observed for the latter reaction) [16]:

$$\begin{bmatrix} Rh^I\text{-A} \\ \rightleftharpoons\ K_{c1} \\ Rh^I\text{-B} \end{bmatrix} + CH_3I \underset{k_{-1}}{\overset{K_1, k_1}{\rightleftharpoons}} \qquad (12)$$

$$\begin{bmatrix} [Rh^{III}\text{-alkyl1A}] & & [Rh^{III}\text{-acyl1A}] & \overset{k_{3A}}{\underset{k_{-3A}}{\rightleftharpoons}} & [Rh^{III}\text{-alkyl2A}] \\ \rightleftharpoons\ K_{c2} & \underset{k_{-2}}{\overset{K_2, k_2}{\rightleftharpoons}} & \rightleftharpoons\ K_{c3} & \overset{k_{3B}}{\underset{k_{-3B}}{\rightleftharpoons}} & \rightleftharpoons\ K_{c4}\ \text{slow} \\ [Rh^{III}\text{-alkyl1B}] & & [Rh^{III}\text{-acyl1B}] & & [Rh^{III}\text{-alkyl2B}] \end{bmatrix}$$

Another result indicative of the fast equilibrium [Rh^{III}–alkyl1 ⇌ Rh^{III}–acyl1] results from a ^{1}H–^{1}H NOESY (Fig. 6), recorded *in situ* during the oxidative addition reaction of **4** to establish the relative dispositions of the CH_3 ligand in the [Rh(bth)(CH_3)(CO)(PPh_3)(I)]–alkyl1 isomers. Irradiation of the CH_3 resonance on the Rh^{III}–alkyl1 isomers (1.6 ppm), resulted in an NOE coupling with the methine, phenyl, PPh_3 and thienyl protons as well as with the methyl signals of Rh^{III}–acyl1 **10A** and **10B** isomers (^{1}H–^{1}H NOESY in Fig. 6). This result is only possible if the CH_3 group of the Rh^{III}–alkyl1 isomers is below (or above) the square planar plane (formed by the two oxygens of the β-diketonato ligands and the other two groups), with the CH_3 group adjacent to the PPh_3 group. The NOE coupling to the methine proton rules out the possibility of the CH_3 group being in a position in the square planar plane. An exceptional result is that as the CH_3 resonances of Rh^{III}–alkyl1 **9A** and **9B** isomers are irradiated, it converts into the Rh^{III}–acyl1 **10A** and **10B** isomers on the time scale of the NMR, showing an increased intensity for the signal of the methyl group on the Rh^{III}–acyl1 isomers at 3.02 and 3.10 ppm. This result is indicative of the fast equilibrium [Rh^{III}–alkyl1 ⇌ Rh^{III}–acyl1].

4. Conclusions

By introducing a thienyl fragment as part of a β-diketonato ligand in the [Rh((C_4H_3S)COCHCOR)(CO)(PPh_3)] complexes with R = C_6H_5 or C_4H_3S, it was possible to provide a general reaction sequence for the oxidative addition of iodomethane to any [Rh^I(L,L′-BID)(CO)(PPh_3)] complex with L,L′-BID = monoanionic bidentate ligand with

donor atoms L and L′. All previously proposed reaction mechanisms for the oxidative addition reaction of CH_3I to a variety of square planar $[Rh^I(L,L'\text{-BID})(CO)(PPh_3)]$ complexes are just special cases of the general mechanism:

$$[Rh^I(L,L'\text{-BID})(CO)(PPh_3)]\ \text{isomers} + CH_3I \underset{k_{-1}}{\overset{K_1, k_1}{\rightleftharpoons}} \text{alkyl1 isomer}$$

$$\text{s} \underset{k_{-2}}{\overset{k_2}{\rightleftharpoons}} \text{acyl1 isomers} \underset{k_{-3}}{\overset{k_3}{\rightleftharpoons}} \text{alkyl2 isomers} \underset{k_{-4}}{\overset{k_4}{\rightleftharpoons}} \text{acyl2 isomers}$$

product for cacsm, hacsm, macsm, macsh, cupf, ox, anmeth, dmavk | **product for acac, tfaa, tfdma, hfaa, tta, sacac** | **product for fctfa, bth, dtm**

The above general mechanism does not distinguish between different rates of isomers. The observed rate of depletion of the two Rh^I isomers of the $[Rh((C_4H_3S)COCHCO(C_6H_5))(CO)(PPh_3)]$ complex containing an unsymmetrical β-diketonato ligand, as well as the observed rate of formation and depletion of the different isomers of each reaction intermediate, are the same, contrary to what was found for the rate of formation of the two $[Rh((C_4H_3S)COCHCOCF_3)(CH_3)(CO)(PPh_3)(I)]$–alkyl2 isomers that formed at different rates [16].

Acknowledgements

Financial assistance by the South African National Research Foundation under Grant No. 2067416 and the Central Research Fund of the University of the Free State are gratefully acknowledged.

References

[1] P.M. Maitlis, A. Haynes, G.J. Sunley, M.J. Howard, J. Chem. Soc., Dalton Trans. (1996) 2187.
[2] K.G. van Aswegen, J.G. Leipoldt, I.M. Potgieter, G.J. Lamprecht, A. Roodt, G.J. van Zyl, Transition Met. Chem. 16 (1991) 369.
[3] P. Braunstein, Y. Chauvin, J. Fischer, H. Olivier, C. Strohmann, D.V. Toronto, New J. Chem. (Nouv. J. Chim.) 24 (2000) 437.
[4] L.J. Damoense, W. Purcell, A. Roodt, J.G. Leipoldt, Rhodium Exp. 5 (1994) 10.
[5] S.S. Basson, J.G. Leipoldt, A. Roodt, J.A. Venter, Inorg. Chim. Acta 128 (1987) 31.
[6] M. Cano, J.V. Heras, M.A. Lobo, E. Pinilla, M.A. Monge, Polyhedron 11 (1992) 2679.
[7] S.S. Basson, J.A. Venter, A. Roodt, in preparation.
[8] J.A. Cabeza, V. Riera, M.A. Villa-Garcia, L. Ouahab, S. Triki, J. Organomet. Chem. 441 (1992) 323.
[9] C.H. Cheng, B.D. Spivack, R. Eisenberg, J. Am. Chem. Soc. 99 (1977) 3003.
[10] L.J. Damoense, W. Purcell, A. Roodt, Rhodium Exp. 14 (1995) 4.
[11] A. Roodt, G.J.J. Steyn, Recent Res. Dev. Inorg. Chem. 2 (2000) 1.
[12] J.G. Leipoldt, S.S. Basson, L.J. Botha, Inorg. Chim. Acta 168 (1990) 215.
[13] G.J.J. Steyn, A. Roodt, J.G. Leipoldt, Rhodium Exp. 1 (1993) 25.
[14] S.S. Basson, J.G. Leipoldt, J.T. Nel, Inorg. Chim. Acta 84 (1984) 167.
[15] S.S. Basson, J.G. Leipoldt, A. Roodt, J.A. Venter, T.J. van der Walt, Inorg. Chim. Acta 119 (1986) 35.
[16] M.M. Conradie, J. Conradie, Inorg. Chim. Acta 361 (2008) 208.
[17] J. Conradie, G.J. Lamprecht, A. Roodt, J.C. Swarts, Polyhedron 23 (2007) 5057.
[18] J.A. Venter, J.G. Leipoldt, R. van Eldik, Inorg. Chem. 30 (1991) 1207.
[19] B.S. Furniss, A.J. Hannaford, P.W.G. Smith, A.R. Tatchell, Vogel's Textbook of Practical Organic Chemistry, 5th ed., John Wiley & Sons, New York, 1994, p. 409.
[20] M.M. Conradie, A.J. Muller, J. Conradie, SA J. Chem. (2008), in press.
[21] (a) Y.S. Varshavskii, T.G. Cherkasova, Russ. J. Inorg. Chem. 12 (1967) 899;
(b) A. Rusina, A.A. Vlcek, Nature (London) 206 (1965) 295.
[22] MINSQ, Least squares parameter Estimation, Version 3.12, MicroMath, 1990.
[23] J.H. Espenson, Chemical Kinetics and Reaction Mechanisms, second ed., McGraw-Hill, New York, 1995, p. 15, 49, 70–75.
[24] J.H. Espenson, Chemical Kinetics and Reaction Mechanisms, second ed., McGraw-Hill, New York, 1995, p. 156.
[25] J. Conradie, G.J. Lamprecht, S. Otto, J.C. Swarts, Inorg. Chim. Acta 328 (2002) 191.